Measuring Fine Structure Splitting in Sodium through Optical Spectroscopy

Gopal K. Goel[*]
MIT Department of Physics
(Dated: April 16, 2023)

We measure the fine structure splitting of energy levels in sodium by observing a doublet structure in the spectrum of sodium gas emission. We provide evidence that the doublet structure does indeed arise from fine splitting. We also compare the measured splitting to theoretical heuristics for the splitting, and find a quantitative match.

I. MOTIVATION

According to the Schrödinger theory of the atom, the electrons are occupying several quantum states, which are distinguished by their energy, angular momentum, spin, etc. *Atomic emission* is the phenomenon where an electron spontaneously transitions from a higher energy state to a lower energy state, thereby releasing a photon with energy exactly equal to the energy difference in the states. By measuring the wavelengths of the emitted light (i.e. finding the peaks of the *emission spectrum* of the atom), we can infer the energy structure of the states of the electrons in the atom.

In particular, we are interested in the *fine structure splitting* of the energy levels, which causes the energy levels of the electron states to come in pairs of values that are extremely close to each other. This effect is caused by the interaction of the spin of the electron with the magnetic field of the nucleus. The splitting is easiest to analyze for hydrogenic atoms (i.e. those with one valence electron), and it is more prominent in heavier atoms. For this reason, we choose to analyze the fine structure splitting in sodium, using optical spectroscopy.

II. THEORETICAL DESCRIPTION

II.1. Review of Hydrogen Atom

We begin by giving a brief overview of fine structure splitting in hydrogen. In hydrogen, we have a single electron electromagnetically interacting with a proton, so the quantum states of the electron are given by solving the Schrödinger equation

$$\mathcal{H}\psi(\vec{r}) := \left(-\frac{\hbar^2}{2m_e}\nabla^2 - \frac{e^2}{4\pi\varepsilon_0 r}\right)\psi(\vec{r}) = E\psi(\vec{r}). \quad (1)$$

Let $\mathbf{L} = \mathbf{r}\times\mathbf{p}$ be the orbital angular momentum operator, $\mathbf{S}$ be the spin angular momentum operator, and $\mathbf{J} = \mathbf{L} + \mathbf{S}$ be the total angular momentum operator. One can show that there is a basis to the solution space of (1) with basis elements parameterized by four quantum numbers $|n, \ell, j, m_j\rangle$ (see §25.6 of [1] for more details). These states have definite energy (given in terms of n), $\mathbf{L}^2$ (given by $\hbar\ell(\ell+1)$), $\mathbf{J}^2$ (given by $\hbar j(j+1)$) and J_z (given by $\hbar m_j$). The quantum numbers must satisfy $n \in \{1, 2, 3, \ldots\}$, $\ell \in \{0, 1, \ldots, n-1\}$, $j \in \{\ell \pm \frac{1}{2}\}$, and $m_j \in \{-j, \ldots, j\}$.

II.2. Fine structure in Hydrogen

The primary source of fine structure correction to the energy levels is the phenomenon of *spin-orbit coupling*, which is due to magnetic interactions between the spin dipole nature of the electron and the magnetic field produced by the nucleus. In the frame of the electron, the nucleus is a moving charge, so the electron feels a magnetic field $\mathbf{B}$. Letting μ be the spin dipole moment of the electron, we see that the hamiltonian needs a correction $\delta H = -\mu \cdot \mathbf{B}$ due to this magnetic interaction. One can show (see §25.7 of [1]) that this correction is given by

$$\delta H = \frac{1}{2mc^2}\frac{1}{r}\frac{\partial V(r)}{\partial r}\mathbf{L}\cdot\mathbf{S},$$

hence the term spin-orbit coupling.

Using the machinery of perturbation theory, one can show that δH contributes an energy correction term that depends only on the values of n, ℓ, j. In particular, states with quantum numbers n and ℓ get divided into two groups based on the value of j (either $\ell + \frac{1}{2}$ or $\ell - \frac{1}{2}$) with a small energy difference given by

$$\Delta E_{n,\ell} = \frac{e^2\alpha^2}{8\pi\varepsilon_0}\frac{1}{n^3\ell(\ell+1)}, \quad (2)$$

where $\alpha \sim \frac{1}{137}$ is the *fine structure constant*.

It is common to label states with the quantum number n followed by one of the letters s,p,d, which correspond to $\ell = 0, 1, 2$, respectively. For example, the state 3s corresponds to $n = 3$ and $\ell = 0$. Sometimes, there may also be a subscript, which corresponds to the value of j. In Figure 1, the energy levels of hydrogen are schematically depicted, specifically the fine structure splitting between levels with the same n and ℓ but different j. One important feature is that the s states don't split, since there is only one value for j, which is $j = \frac{1}{2}$.

---

[*] gopalkg@mit.edu

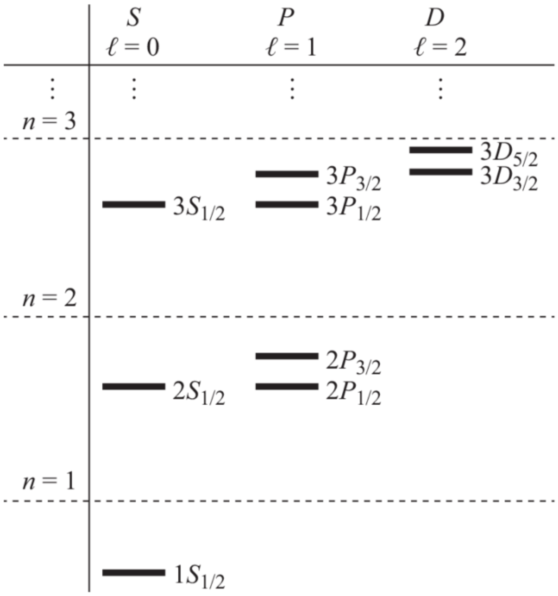

FIG. 1. Schematic diagram of the energy levels of hydrogen with fine structure splitting (not shown to scale)

II.3. Fine structure in Sodium

The fine structure splitting in sodium follows the same general patterns, but there is no exact formula like (2). The $n = 1$ and $n = 2$ shells are full in sodium, so the singular valence electron has physics somewhat similar to a hydrogen electron, due to shielding from the inner layers. The ground state is now 3s, again because the inner shells are full.

We heuristically expect the splitting to follow the same form as (2), so in particular, we expect

$$\Delta E_{n,\ell} \sim \frac{1}{n^3 \ell(\ell+1)}. \tag{3}$$

We choose to analyze fine structure splitting in sodium since the splitting in hydrogen is too small for our apparatus to detect (less than 0.1 Å).

III. EXPERIMENTAL GOALS

Our first goal is to measure a spectrum of sodium, and observe that the emission peaks come in doublets, which corresponds to the fine structure splitting in the states that are being transitioned to and from. We also aim to identify the state transitions that lead to those peak doublets.

Our second goal is to verify that the energy difference in the two peaks corresponding to a transition from state X to state Y is the same as the energy difference in the two peaks corresponding to a transition from state Y to state Z. Here we are assuming that the fine structure splitting in state Y is much larger than in states X and Z. Verifying this would provide evidence for the hypothesis that the observed doublets indeed arise from fine structure splitting in the individual states.

Our third and final goal is to verify that the fine structure splitting in a state (n, ℓ) is approximately proportional to $\frac{1}{n^3\ell(\ell+1)}$.

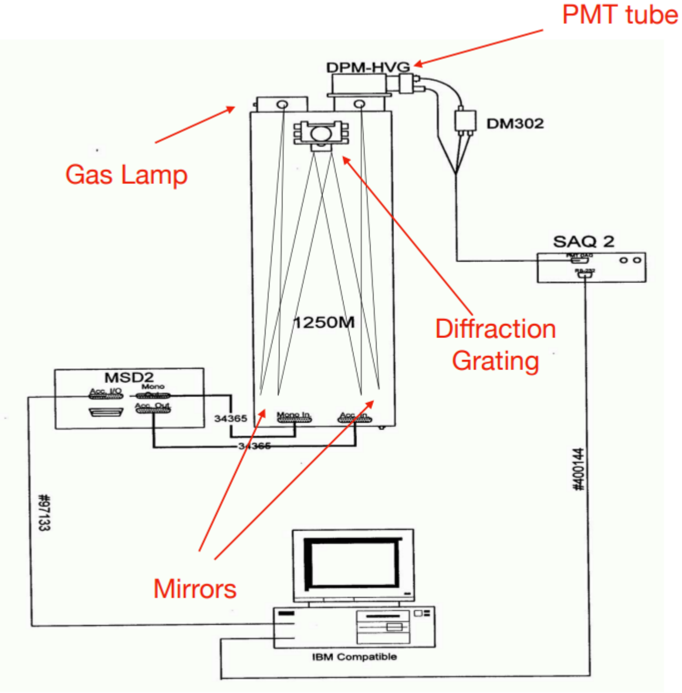

FIG. 2. Monochromator schematic setup ([5])

IV. EXPERIMENTAL PROCEDURE

IV.1. Experimental Setup

We measure the emission spectrum of an atomic gas using a monochromator. The experimental setup is depicted in Figure 2.

Light from atomic emission leaves the gas lamp, and is passed through a thin slit as it enters the monochromator. The light is then collimated by a circular mirror at the other end of the monochromator onto a diffraction grating, which splits the different wavelengths of the light into beams of slightly varying angles. The different beams are then focused through another circular mirror, and are sent to the photomultiplier tube (PMT), passing through another slit in the process. Due to the diffraction grating splitting the different wavelengths of light into beams of different angles, only a small band of wavelengths makes it to the PMT, which allows us to measure the intensity of a specific wavelength in the emission spectrum.

We have the ability to tune the angle of the diffraction

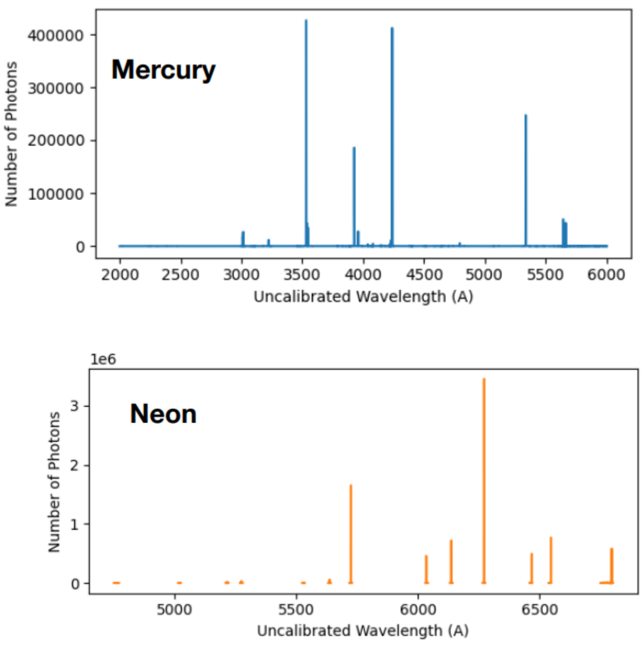

FIG. 3. Measured spectra of mercury and neon

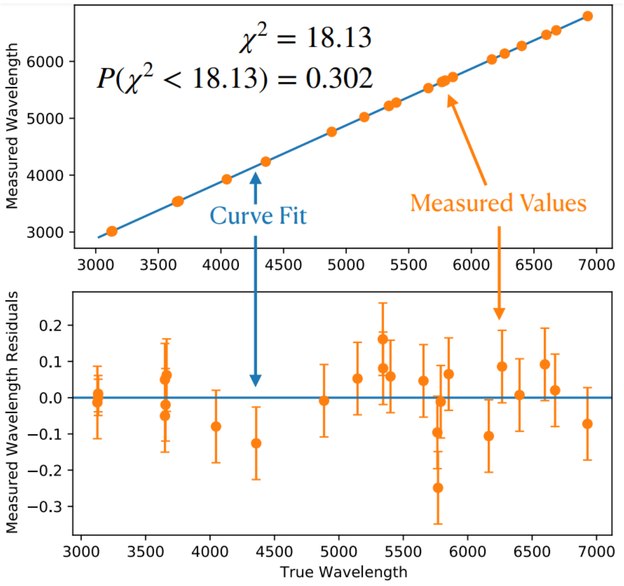

FIG. 4. Calibration curve fitting with χ^2 probability and residuals

grating, which allows us to send different wavelengths of light into the PMT tube. We can also tune the slit width, and in particular decreasing the slit width decreases the band of wavelengths that make it to the PMT (thereby increasing the resolution of our measurement), but also decrease the amount of signal the PMT picks up. For almost all scans, we keep the slit width fixed at 10μ.

We control the angle of the diffraction grating through software, and we also read the photon count value (PMT reading) as a function of wavelength from software. The software automatically converts the angle of the diffraction grating into a value for the measured wavelength, but over several runs, the conversion is off, and has a large systematic offset. A large part of this experiment is getting rid of that systematic offset by calibrating the wavelength readings by comparing to known emission spectra for neon and mercury.

IV.2. Wavelength Calibration

As mentioned above, the software outputs photon count as a function of wavelength, but the wavelengths are uncalibrated. We solve this by measuring the spectra of mercury and neon using our setup, and comparing to known values (found at [2], [3]), and computing a calibration function which allows us to convert measured wavelength λ_m into true wavelength λ_t.

Figure 3 shows the measured spectra of mercury and neon. Given that the uncalibrated wavelengths are somewhat close to the true values, we can construct a bijection between our measured peaks and the true peaks. It is particularly useful to use doublets in the spectrum, for example, the doublet near 3130 Åin mercury was particularly useful in matching the peaks.

The mercury peaks generally cover the range $[3000, 6000]$ Åand the neon peaks cover the range $[5000, 7000]$ Å, so using both sets of peaks gives us a wide range we can interpolate in. We extract a set of 24 peaks that we use for our calibration.

We use a quadratic fit

$$\lambda_m = a\lambda_t^2 + b\lambda_t + c \tag{4}$$

with χ^2 curve-fitting. The result of the curve fit is shown in Figure 4. The fit parameters are $a = (-4.56 \pm 0.15) \cdot 10^{-7}\,\text{Å}^{-1}$, $b = 1.0004 \pm 0.0001$, and $c = -114.1 \pm 0.3\,\text{Å}$. We also keep track of the covariance matrix of the fit parameters, which will be important for error propagation later.

V. ANALYSIS AND RESULTS

V.1. Raw Data and Calibration

We measure three doublet pairs in the sodium spectrum, with uncalibrated wavelengths given by

$$3184.6, 3185.2, 5762.35, 5768.25, 8040.3, 8051.85,$$

all in Å, and with uncertainties of 0.2 Å(given by estimating the peak width). The raw spectra are shown in Figure 5.

We now calibrate these wavelengths using our fit function. In order to estimate the uncertainties on the calibrated wavelengths, we draw each of the three fit parameters a, b, c from a multivariate Gaussian with the

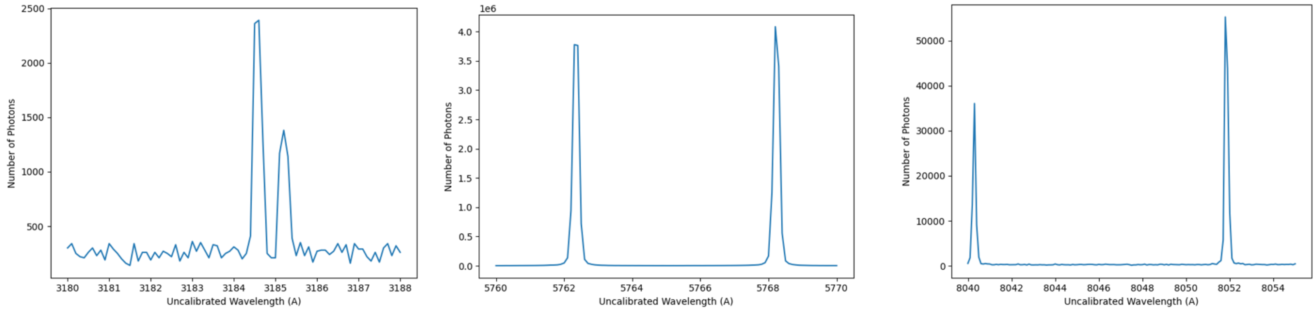

FIG. 5. Measured spectra for three sodium doublets

right mean and covariance, and we randomly sample the calibrated values 1000 times, and take the standard deviation of those samplings to be the uncertainty on the calibrated values.

Performing the calibration, we find calibrated wavelengths of

$$\begin{aligned}
4p \to 3s: &\quad [3302.3 \pm 0.6]\,\mathring{A}, \quad [3302.9 \pm 0.6]\,\mathring{A}\\
3p \to 3s: &\quad [5889.9 \pm 1.1]\,\mathring{A}, \quad [5895.8 \pm 1.1]\,\mathring{A}\\
3d \to 3p: &\quad [8181.6 \pm 1.6]\,\mathring{A}, \quad [8193.4 \pm 1.6]\,\mathring{A}.
\end{aligned}$$

Here, we match the emission wavelengths to state transitions by comparing to the known sodium spectrum found at [4].

The inverse wavelength is proportional to the energy, so we report the difference in inverse wavelengths for each doublet as a proxy for the energy difference. The inverse wavelength differences from the three transitions are shown in Figure 6, measured in $10^{-7}\,\mathring{A}^{-1}$. Note that the errors in the above reported wavelengths are highly correlated, so to compute the errors in the inverse wavelength difference we resample the fit parameters and report the standard deviation of the inverse wavelength difference as the uncertainty.

V.2. Discussion of Results

In the above, we achieved our first experimental goal of measuring the doublet peaks and identifying their state transitions.

Note that we have two transitions that share an endpoint, which are $3d \to 3p$ and $3p \to 3s$. The level $3s$ has no splitting, and the splitting of level $3d$ is much smaller than that of $3p$, due to the heuristic (3). We observe that their inverse wavelength differences are equal within their errors, so our second experimental goal has also been achieved.

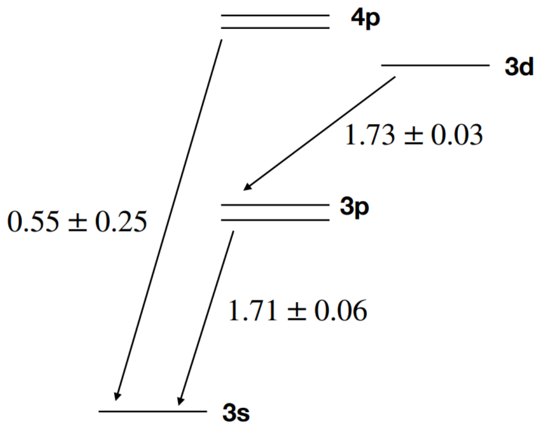

FIG. 6. Inverse wavelength differences for various transitions in sodium, measured in $10^{-7}\,\mathring{A}^{-1}$

Using the $4p \to 3s$ transition, we can estimate the energy splitting of the $4p$ level to be $[0.55 \pm 0.25] \times 10^{-7}\,\mathring{A}^{-1}$, and we can estimate the splitting of the $3p$ level to be $[1.72 \pm 0.05] \times 10^{-7}\,\mathring{A}^{-1}$. These have ratio 0.3 ± 0.1, and the heuristic (3) predicts a ratio $3^3/4^3 = 0.42$, again within error of our measurement. This achieves our third experimental goal.

V.3. Discussion of Systematic Uncertainty

The primary source of systematic uncertainty is the calibration of the instrument, which we attempted to minimize by performing an elaborate calibration procedure. The second main source of systematic uncertainty is lack of persistence of calibration day to day. We have measurements of the mercury spectrum separated by five days, and we find that the difference in peak values is always within $0.1\,\mathring{A}$, so this systematic uncertainty is dwarfed by the statistical uncertainty.

ACKNOWLEDGEMENTS

Thanks to my partner O. Dugan, and all the JLab staff, particularly Dr. Levine and Dr. Robinson.

[1] *Mastering Quantum Mechanics*, MIT Press (2022).

[2] *Strong Lines of Mercury*, NIST, `https://physics.nist.gov/PhysRefData/Handbook/Tables/mercurytable2.htm`

[3] *Strong Lines of Neon*, NIST, `https://physics.nist.gov/PhysRefData/Handbook/Tables/neontable2.htm`

[4] *Strong Lines of Sodium*, NIST, `https://physics.nist.gov/PhysRefData/Handbook/Tables/sodiumtable2.htm`

[5] *Optical Spectroscopy of Hydrogenic Atoms*, MIT Department of Physics (2017).